# Shape matters: Highly selective antimicrobial bottle brush copolymers via a one-pot RAFT polymerization approach

Anne-Catherine Lehnen,[a,b] Alain M. Bapolisi,[a] Melanie Krass,[c] Ahmad AlSawaf,[a] Jan Kurki,[a] Sebastian Kersting,[d] Hendrik Fuchs,[c] Matthias Hartlieb[*,a,b]

a Institute of Chemistry, University of Potsdam, Karl-Liebknecht-Straße 24-25, 14476, Potsdam, Germany
b Fraunhofer Institute for Applied Polymer Research (IAP), Geiselbergstraße 69, 14476, Potsdam, Germany
c Charité – Universitätsmedizin Berlin, corporate member of Freie Universität Berlin and Humboldt-Universität zu Berlin, Institute of Diagnostic Laboratory Medicine, Clinical Chemistry and Pathobiochemistry.
d Fraunhofer Institute for Cell Therapy and Immunology (IZI), Am Mühlenberg 13, 14476, Potsdam, Germany

* Correspondence to mhartlieb@uni-potsdam.de

**Abstract**

The one-pot synthesis of antimicrobial bottle brush copolymers is presented. RAFT polymerization is used for production of the polymeric backbone, as well as for the grafts, which were installed using a grafting from approach. A combination of *N*-iso propyl acrylamide and a Boc protected primary amine-containing acrylamide was used in different composition. After deprotection polymers featuring different charge densities were obtained in both, linear and bottle brush topology. Antimicrobial activity was tested against three clinically relevant bacteria strains and growth inhibition was significantly increased in bottle brush copolymers. Blood compatibility investigations revealed strong hemagglutination for linear copolymers and pronounced hemolysis for bottle brush copolymers. However, one bottle brush copolymer with a 50% charge density strong antibacterial activity and negligible blood toxicity resulting in selectivity values as high as 320. Membrane models were used to probe the mechanism of shown polymers, which was found to be based on membrane disruption. The trends from biology are accurately reflected in model systems indicating that differences in lipid composition are responsible for selectivity. However, bottle brush copolymers were found to possess increased cytotoxicity against HEK cells when compared with linear analogues. The introduced synthetic platform enables screening of further parameters associated to bottle brush copolymers, which might lead to even better activity profiles.

**Introduction**

Antimicrobial resistance (AMR) is an increasingly serious problem to our society and the World Health Organization asserted it to one of humanities top 10 global public health threats.[1] The non-therapeutic and overuse of antibiotics leads to an increasing number of bacteria which are resistant against these drugs.[2, 3] Through the loss of effective antibiotics, also many advantages of modern medicine are in jeopardy, as resistant bacteria endanger immune compromised patients among others.[4, 5]

One possible solution for this problem are antimicrobial polymers (AP)s.[6, 7] These macromolecules are able to kill bacteria through interaction with the cellular membrane of the microorganism.[8-10] A typical AP possesses cationic and hydrophobic building blocks. The cationic units interact with the negatively charged lipid bilayer of the bacterial cell envelop through electrostatic interactions. Upon binding to the cell, the hydrophobic component of the AP inserts itself into the membrane causing disruption and cell death.[11, 12]

Because of the non-specific nature of this interaction between the polymer and the bilayer, the development of a resistances against APs is far less likely when compared to common antibiotics.[7, 13] Here, small genetic adaptions are usually sufficient to develop a resistance,[14] e.g. via efflux pumps [15] or target alteration.[16] However, these strategies are inefficient against APs, and it was shown that cultivating bacteria in the presence of sub-lethal concentrations of APs does not result in a change of the minimum inhibitory concentration (MIC).[7, 17]

Different parameters can influence the antimicrobial activity and toxicity of APs. Common factors to regulate the selectivity of antimicrobial materials are for example the amphiphilic balance,[18-21] or the used type of cations. [19, 22-25] In addition, the polymer topology is an important factor which influences the properties of APs.

Antimicrobial macromolecules can be designed to have different structures, such as block[7, 17, 26, 27], star shaped[28, 29] or bottle brush copolymers.[30, 31] Our previous work has shown that an APs with a bottle brush architecture possess lower blood toxicity, and a higher antibacterial activity, compared to linear polymers with the same composition.[30]

However, the previously used strategy to first synthesize side chains featuring norbornene functionalities via reversible addition-fragmentation chain-transfer (RAFT) polymerization, and subsequently produce bottle brushes via a grafting-through approach, by polymerizing the norbornene groups with ring-opening metathesis polymerization (ROMP) had certain disadvantages. It was difficult to control parameters like side chains length, the length of the bottle brushes, and also the grafting density could not be varied in a straightforward way.

For this reason, a new route to synthesize antimicrobial bottle brushes was developed within this contribution, enabling straightforward access to structural variation in an easy process. To produce bottle brush copolymers with controlled backbone and side chain length, RAFT polymerization was used for both polymerization steps. This polymerization technique was chosen because it is a versatile and robust method to synthesis highly functional polymers in a controlled manner.[7, 32-34] To overcome previous limitation a grafting-from approach was used to synthesis antimicrobial bottle brushes. (**Scheme 1**)

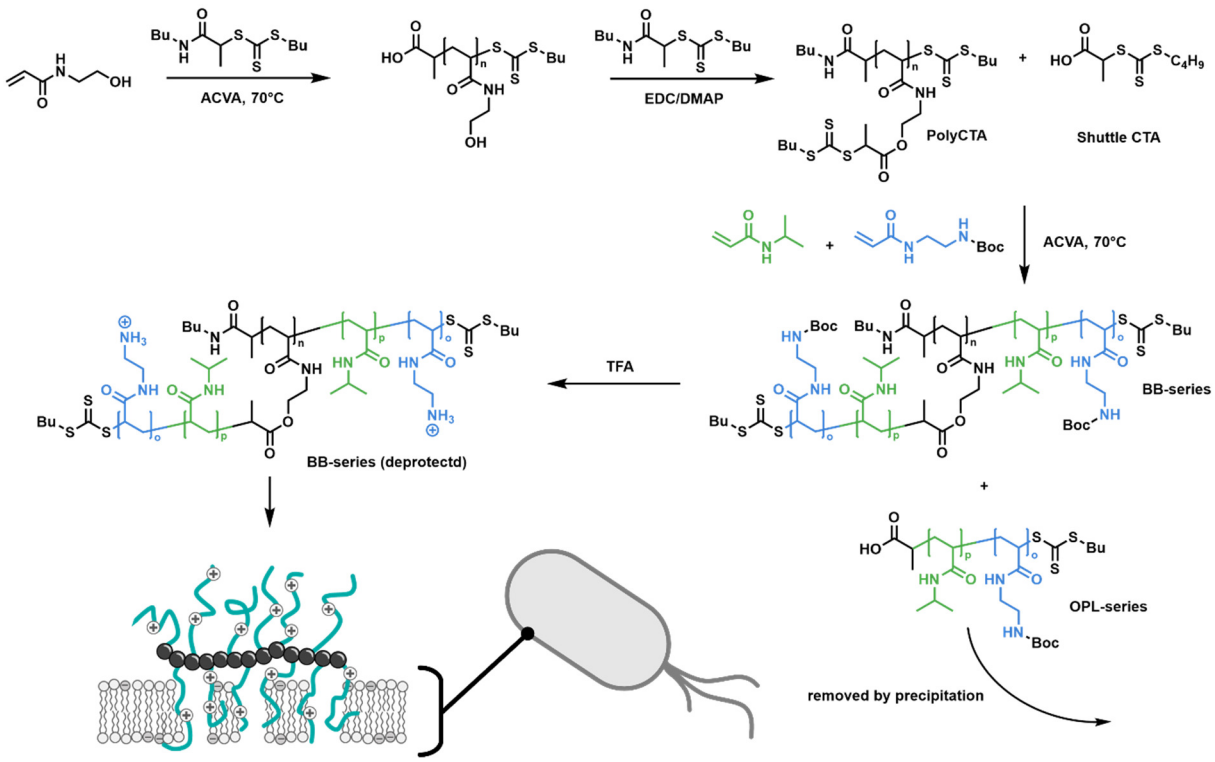


**Scheme 1**: Schematic representation of the one-pot synthesis of antimicrobial bottle brushes via an all-RAFT polymerization strategy, as well as the proposed interaction with bacterial cellular membranes

By the use of a grafting-from strategy it is possible to vary side chains length and length of the polymeric backbone independent of each other.[33, 35, 36] It was shown that it is possible to synthesis complex bottle brush architectures via a combination of grafting-from and RAFT polymerization.[33]

The general strategy, which was used in this report is the synthesis of a polymeric backbone in a first polymerization step, followed by the functionalization of this polymer with chain-transfer agents (CTA)s to obtain a polyCTA. In a second RAFT polymerization, grafted side chains are generated by a grafting-from method. Here, cationic and hydrophobic units were introduced into the side polymer to produce polymeric bottle brushes which are antimicrobial active.

To achieve a beneficial amphiphilic balance *N*-isopropyl acrylamide (NIPAM) and *N*-tertbutoxycarbonyl-amino ethyl acrylamide (BocAEAM) were used, where NIPAM acts as the hydrophobic part which enables membrane disruption, and BocAEAM after deprotection possesses primary amine groups, which can interact with the cellular membrane of bacteria. To develop a method to synthesize antimicrobial bottle brushes as easy and modular as possible, a one-pot approach via RAFT polymerization, where only the final polymer needs to be purified via precipitation before deprotection was pursued.

In addition, the positive influence of the bottle brush architecture for applications as therapeutical antimicrobial agents should be shown. Therefore, the materials demand low cytotoxicity, in particular against red blood cells combined with high antimicrobial activity. As shown before, the structure of APs influences their performance. [17, 28, 30] To have a closer look

to this parameter the antimicrobial activity and hemotoxicity of bottle brush copolymers, as well as their interaction with artificial membrane models will be compared to linear statistical copolymers, which mimic the side chains of the tested bottle brushes.

**Results and Discussion**

To create a synthetic strategy where different parameters like side chain length, grafting density or the composition of the side chains can be easily varied a grafting-from methodology in a one-pot approach was chosen. This strategy gives advantages like simple reaction conditions, no purification between reaction steps while respective polymerization reactions are still controlled.

To produce bottle brush copolymers using the one-pot strategy outlined in **Scheme 1**, the first step was to synthesize the polymeric backbone. Therefore, 2-Hydroxyethylacrylamide (HEAm) was selected, because the hydroxy group of the monomer gives the opportunity to functionalize the backbone with a CTA in a subsequent reaction step to produce a PolyCTA. Dimethylformamide (DMF) was found to be ideal as a solvent, as it is able to dissolve all educts and products during the one-pot procedure.

Trithiocarbonates are typical CTAs for RAFT polymerizations, often featuring an R-group containing a carboxylic acid function.[37, 38] However, such a CTA would lead to side reaction while coupling the CTA to the polymeric backbone via an esterification reaction to obtain a PolyCTA. To avoid inadvertent coupling, an amine was coupled to propanoic acid butly trithio carbonate (PABTC) to deactivate the carboxylic acid (**Scheme S1**). Through this reaction butyl (1-(butyl amino)-1-oxopropan-2-yl) carbonotrithioate (Amid-PABTC) was synthesized, a CTA which is able to control polymerization of the backbone while being inactive in esterification reactions. The success of this coupling was determined via $^{1}$H-NMR spectroscopy (**Figure S1**).

Using Amid-PABTC as CTA in a RAFT-polymerization process, a well-defined pHEAm could be obtained with a dispersity of 1.41 (Figure 1). The polymerization was performed using 4,4'-Azobis(4-cyanopentanoic acid) (ACVA) as an initiator at 85 °C for 4 h, and conversion was found to be quantitative (96%). Purification was not necessary, which is an important prerequisite for the outlined strategy. As mentioned before a Steglich-like esterification with 1-Ethyl-3-(3-dimethylaminopropyl) carbodiimide hydrochloride (EDC-HCl) and 4-Dimethylaminopyridine (DMAP) as coupling reagents was used to connect, the carboxylic group of PABTC with the hydroxy group of pHEAm backbone. While PABTC was used in an excess to ensure quantitative functionalization, non-consumed CTA can be left in the reaction mixture as it can be used as a shuttle CTA.[39] The use of a shuttle CTA is necessary as synthesizing bottle brushes via the grafting-from approach from a linear backbone with high density of bound CTA functionalities can lead to undesired coupling reactions, when the CTA is bound via its R-group. In addition, the active radicals are often trapped within their individual polymer bottle brush and cannot efficiently be transferred between brushes, limiting molecular weight control. More importantly, driving the reaction to high conversions will lead to brush-brush coupling, severely increasing dispersity. Through the use of a shuttle CTA these problems can be overcome, as radicals are transferred between brushes and bimolecular termination does not necessarily lead to brush-brush coupling, as first described

by Müller and coworkers.[39-41] Beside its positive influence on polymerization control, the use of a shuttle CTA has the advantage that simultaneously linear polymer chains are produced, which mimic the side chains of the bottle brushes, and can be analyzed separately, thus giving an impression of the molecular weight distribution of grafted chains.[33] To analyze the different intermediate steps $^{1}$H-NMR and size exclusion chromatography (SEC) was used. In $^{1}$H-NMR spectroscopy, the success of backbone functionalization can be seen by the disappearance of the signal of the $CH_2$-group (at 3.58 ppm) which is adjacent to hydroxyl group (**Figure 1**). This indicates near quantitative functionalization of monomer units and a high grafting density. In addition, SEC analysis shows promising results for the functionalization step, as a PolyCTA was produced with a monomodal SEC curve and a dispersity of 1.38. Also, a clear shift to higher molar mass can be seen in comparison to polymeric backbone.

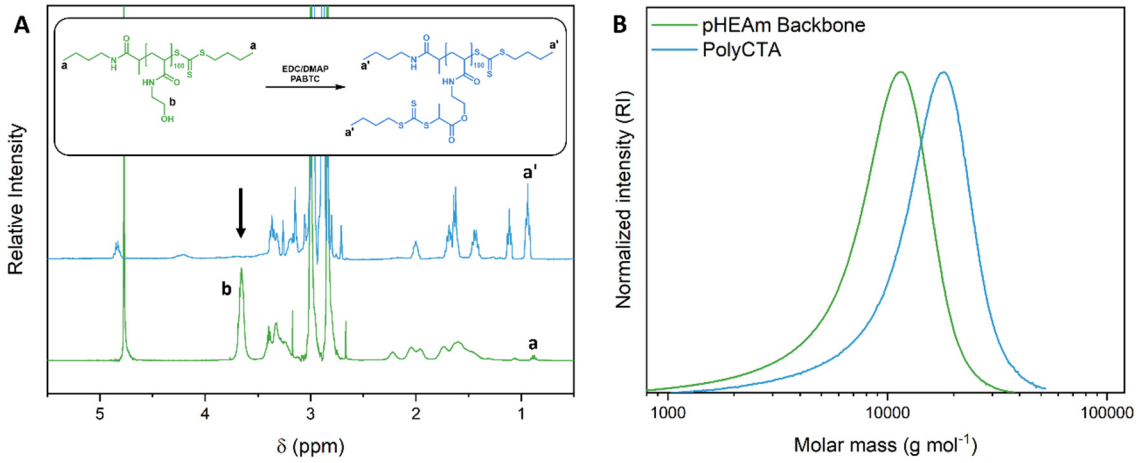


**Figure 1**: Comparison between pHEAm backbone and PolyCTA. A) $^{1}$H-NMR spectra (solvent was $D_2O$ and $CDCl_3$) Black mark: Illustrating disappearance of the signal of $CH_2$ group which was next to hydroxy group within the polymeric backbone to demonstrate the success of PABTC functionalization. B) SEC curves (Eluent was NMP at 60 °C, using a poly(styrene) calibration).

With the synthesized PolyCTA it was possible to graft side chains directly from the backbone and therefore to vary properties like side chain length or composition. To probe this ability, bottle brush copolymers were synthesized using only NIPAM and later with statistical pNIPAM-*stat*-BocAEAM copolymer side chains, using ACVA at 85 °C for 4 h. To prove that it is possible to vary side chain length three bottle brushes were synthesized with pNIPAM side chains and a degree of polymerization (DP) of 10, 20 or 30 respectively. As it can be seen in the SEC graphs (Figure 2) a clear increase in molar mass can be identified with increasing side chain length. While the curves are monomodal and the dispersity is below 1.25.

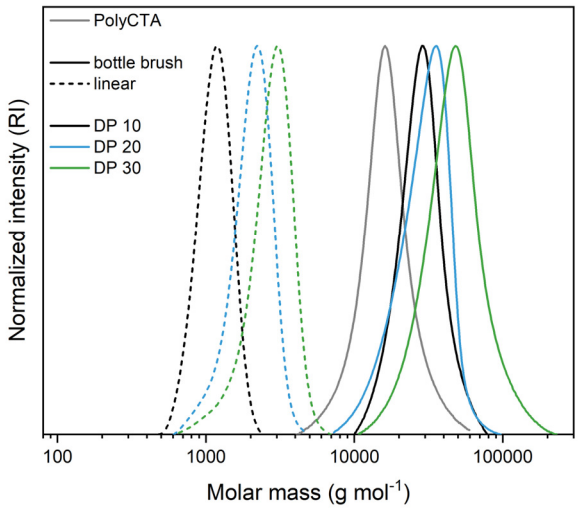


**Figure 2**: SEC traces of bottle brush copolymers and linear polymers featuring pNIPAM side chains with different graft lengths. THF was used as an eluent and a PS calibration was used.

The next step was to synthesize antimicrobial bottle brushes using the produced polyCTA. As the amphiphilic balance is the most important parameter in the design of antimicrobial polymers, various comonomer ratios were targeted. To limit the number of samples, side chain length was kept constant to DP 20. Therefore, statistical copolymer side chains were targeted with different ratios of BocAEAM and NIPAM (BB-series). To optimize antimicrobial activity and toxicity the composition was varied between 20 % to 70 % of cationic subunits. NIPAM was used as hydrophobic comonomer, with a comparable low hydrophobicity and mimicking the structure of the amino acid leucine. Previous studies have shown that NIPAM is well suited for such applications due to the resulting low toxicity.[7, 30] RAFT polymerization was performed using ACVA as initiator at a temperature of 85 °C for 4 h achieving near quantitative conversion (> 95 %) in each case.

After this polymerization step the linear chains can be separated from the bottle brush via a simple precipitation, as linear chains can be solubilized in cold diethyl ether while bottle brush copolymers are insoluble in this medium. After deprotection of cationic units using trifluoroacetic acid (TFA) the final antimicrobial bottle brushes were obtained. Success of the deprotection reaction was verified via $^{1}$H-NMR spectra by disappearance of the methyl signal, which is associated with Boc protection group (Figure S2). The overall process was well-controlled resulting in low dispersed brush copolymers and linear chains (Table 1).

Table 1: Analytical Data of Bottle Brush Copolymers

| | | | Ratio (NIPAM:BocAEAm) | | before deprotection[a] | | after deprotection | | | | | |
|---|---|---|---|---|---|---|---|---|---|---|---|---|
| | | | | | | | PEG calibr.[b] | | | MALLS calibr. [b] | | |
| Sample | Conversion (%) | Graft DP[c] | theor. | measured | $M_n$ (g mol$^{-1}$) | Đ | $M_n$ (g mol$^{-1}$) | Đ | | $M_n$ (g mol$^{-1}$) | Đ | |

| | | | | | | | | | | |
|---|---|---|---|---|---|---|---|---|---|---|
| **Bottle brush copoylmers** | | | | | | | | | | |
| BB 20 | 93 | 14 | 80:20 | 79:21 | 30,500 | 1.16 | 43,500 | 1.17 | 524,300 | 2.47 |
| BB 30 | 95 | 14 | 70:30 | 71:29 | 31,600 | 1.16 | 50,800 | 1.20 | 180,900 | 1.01 |
| BB 40 | 96 | 13 | 60:40 | 62:38 | 36,400 | 1.18 | 57,300 | 1.23 | 173,300 | 1.02 |
| BB 50 | 97 | 17 | 50:50 | 53:47 | 18,400 | 1.15 | 43,900 | 1.22 | 102,500 | 2.14 |
| BB 60 | 95 | 16 | 40:60 | 43:57 | 21,500 | 1.14 | 44,800 | 1.22 | 125,200 | 1.28 |
| BB 70 | 97 | 19 | 30:70 | 32:68 | 26,200 | 1.14 | 47,400 | 1.18 | 166,900 | 1.02 |
| **Linear chains (from one pot approach)** | | | | | | | | | | |
| OPL 20 | 93 | 14 | 80:20 | 79:21 | 2,000 | 1.12 | - | - | | |
| OPL 30 | 95 | 14 | 70:30 | 71:29 | 2,300 | 1.11 | - | - | | |
| OPL 40 | 96 | 13 | 60:40 | 62:38 | 2,400 | 1.11 | - | - | | |
| OPL 50 | 97 | 17 | 50:50 | 53:47 | 2,400 | 1.13 | - | - | | |
| OPL 60 | 95 | 16 | 40:60 | 43:57 | 2,500 | 1.13 | - | - | | |
| OPL 70 | 97 | 19 | 30:70 | 32:68 | 2,700 | 1.07 | - | - | | |
| **Linear chains (synthesized separately)** | | | | | | | | | | |
| L 20 | 98 | 18 | 80:20 | 78:22 | 2,200 | 1.13 | 2,200 | 1.34 | | |
| L 30 | 96 | 18 | 70:30 | 67:33 | 2,300 | 1.13 | 2,600 | 1.36 | | |
| L 40 | 97 | 19 | 60:40 | 58:42 | 2,600 | 1.09 | 3,500 | 1.28 | | |
| L 50 | 96 | 20 | 50:50 | 50:50 | 2,600 | 1.12 | 3,800 | 1.21 | | |
| L 60 | 95 | 18 | 40:60 | 39:61 | 3,500 | 1.30 | 4,300 | 1.19 | | |
| L 70 | 95 | 18 | 30:70 | 33:67 | 3,600 | 1.29 | 5,000 | 1.16 | | |

[a] In THF using a PS-calibration.
[b] The Eluent was water with 0.1 M NaCl and 0.3 V% formic acid using a PEG-calibration or MALLS calibration.
[c] Determined via $^1$H-NMR in $CDCl_3$

While it was easy to separate bottle brush copolymers from the residual reaction solution, the purification of respective linear chains (OPL-series) from DMF proved to be difficult. Data from $^1$ H-NMR and SEC analysis of OPL directly from reaction solution are still presented in **Table 1** as definition of shuttle chains is indicative of grafted side chains in bottle brushes. However, for later biological tests a separate set of linear chains was produced separately in a different solvent (dioxane, L-series). Comparison of respective data on molecular weight and composition before deprotection shows a high degree of similarity. (**Figure S3**, **Table S1&2**).

The composition of synthesized copolymers was determined by $^1$H-NMR spectroscopy comparing the signals of the Boc protection group (BocAEAm) with the methyl signal of NIPAM (**Figure S2**). The obtained monomer ratios match closely with the feed ratios of the polymerization indicating successful copolymerization reactions. The composition of BB and OPL were determined from the crude reaction solution and are therefore identical. Data obtained from the L-series are comparable with minor deviations.

Also, after deprotection $^1$H-NMR spectra were recorded to probe if monomer ratios match with previous data. Therefore, the signals of the two alkyl groups between the secondary amine and the ammonium group was compared with the methyl signals of NIPAM. It could be seen that also after deprotection the ratios are comparable between the L- and the BB-series and are nearly identical to the measured values which were obtain before deprotection step with marginal deviations (**Table S3**).

Initial analysis of molecular weight distribution of protected copolymers was performed from reaction solution of protected polymers using THF as eluent (**Figure S4**). While the targeted graft length was held constant, linear chains show a small increase in $M_n$ with increasing

content of BocAEAm, a trend that has been observed before.[30] Still, all values are in the same range and dispersity is low (< 1.2). As expected, respective bottle brush copolymers show significantly increased molecular weight. Here, no obvious trend regarding the molecular weight can be observed. It should however be noted that measurements were calibrated with a linear standard (poly(styrene)) which does not accurately reflect the grafted nature of the BB-series. Also, comparison between OPL and L series shows a high degree of similarity (**Figure S3**).

Because the counterion can influence the properties of bottle brushes[42] it was necessary to exchange the TFA counterion by a chloride ion. Therefore, aqueous solutions of bottle brush copolymers were prepared, and dialyzed against sodium chloride solution (0.1 M), a diluted aqueous solution of HCl (pH = 4), and finally deionized water ($3.7 \cdot 10^{-4}$ mol $L^{-1}$) via ultra-filtration (10kDa MWCO). During this process all residual small molecules and linear chains were washed out. Acidification was necessary, as otherwise primary amine groups could react with the terminal trithiocarbonate groups and create thiol functionalities via aminolysis, which in turn could lead to gelation under presence of oxygen. When comparing SEC curves of the bottle brushes which were measured directly after the exchange of counterion and SEC curves which were recorded one month later, it can be seen that cross linking was suppressed effectively (**Figure S5**).

To exchange counterion within the L-series ion exchange resin beads (AmberLite® HPR4800 Cl) were used. Hence, the linear polymers were dissolved in water (31.5 mol $L^{-1}$) and filtered through the resin. Afterwards the solvent was removed under reduced pressure.

After deprotection it was possible to analyze copolymers using an aqueous SEC setup. The acidic eluent (0.3V % formic acid and 0.1M NaCl) was ideally suited for cationic polymers. The SEC curves of the deprotected bottle brushes and linear chains are shown in **Figure 3**. Obtained curves are unimodal, indicating the absence of unwanted side reactions (e.g., aminolysis) during deprotection and purification. As linear chains produced during bottle brush synthesis were not purified, deprotection and SEC analysis was not attempted. Deprotected bottle brush copolymers show excellent definition, comparable to values obtained before deprotection. Again, the molecular weight is similar for all members of the BB-series. Linear chains showed increased dispersities, which could however be associated to the PEG calibration that might not accurately reflect chain in lower size regime. The unimodal nature of the curves indicates absence of chain coupling during deprotection (**Figure 3**). Also here, monomer ratio seems to influence hydrodynamic behavior significantly for linear chains, as indicated by increasing molecular weight within the series. Overall, cationic bottle brush copolymers could be synthesized in a one-pot procedure in high definition.

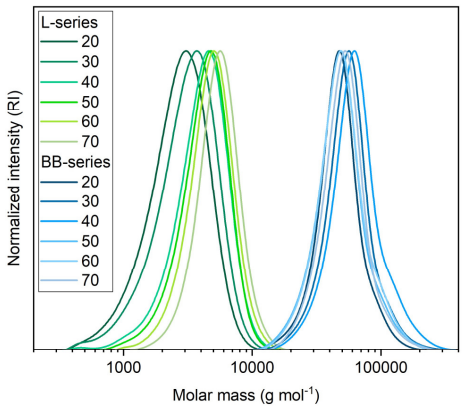


**Figure 3**: Comparison of SEC curves of bottle brush and statistical copolymers with varying composition. The eluent was water with 0.1M NaCl + 0.3 V% formic acid and a PEG calibration was used.

To test antimicrobial activity of the produced polymers and investigate the influence of polymer topology and composition, the minimum inhibitory concentration (MIC) against gram-negative and gram-positive bacteria was determined (**Figure 4**, **Table 2**, **Figure S6**). As gram negative strains *Escherichia coli* (E. coli) and *Pseudomonas aeruginosa* (P. aeruginosa) were used and a methicillin and oxacillin resistant strain of *Staphylococcus aureus* (MRSA) as a gram-positive example. Using MRSA it can be shown that the synthesized polymers are effective against bacteria which have developed resistances to conventional antibiotics. E. coli was chosen as it represents a common strain in hospitals (for example in catheter infection), and P. aeruginosa as it was listed 2017 by the WHO as one critical pathogens were research and development of new antibiotics needed.[43]

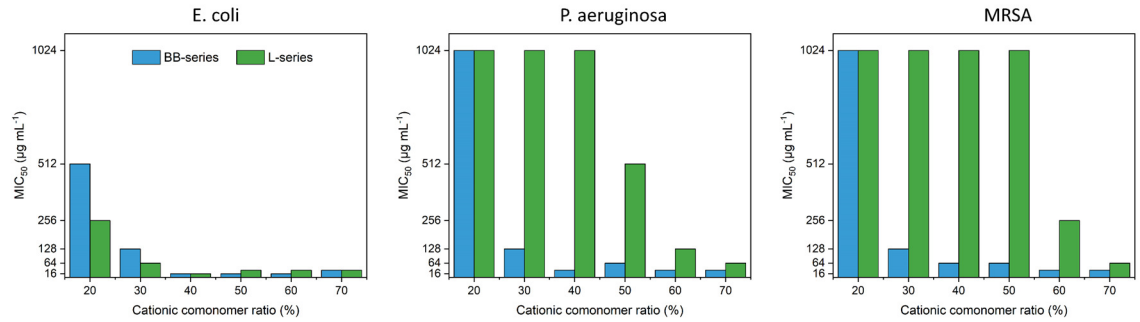


**Figure 4**: Comparison of MIC values of different antimicrobial polymers against three bacterial strains depending on their polymer architecture.

**Table 2**: Biological activity and hemocompatibility of bottle brush and linear copolymers.

| Topology | Cationic comonomer content (%) | MIC (μg mL$^{-1}$) | | | Hemocompatibility (μg mL$^{-1}$) | | Selectivity[d] | | | $IC_{50}$ (μg mL$^{-1}$) |
|---|---|---|---|---|---|---|---|---|---|---|
| | | EC[a] | PA[a] | MRSA | $Hc_{10}$ | $c_H$[c] | EC[a] | PA[a] | MRSA | |
| **BB-series** | 20 | 520 | 1024 | >1024 | < 40 | > 5120 | < 0.08 | < 0.04 | < 0.04 | 35 |
| | 30 | 128 | 128 | 128 | < 40 | > 5120 | < 0.31 | < 0.31 | < 0.31 | 56 |
| | 40 | 16 | 32 | 64 | 80 | > 5120 | 5 | 2.5 | 1.25 | 62 |
| | 50 | 16 | 64 | 64 | > 5120 | > 5120 | > 320 | > 80 | > 80 | 151 |
| | 60 | 16 | 32 | 32 | 640 | 5120 | 40 | 20 | 20 | 22 |
| **L-series** | 30 | 32 | 32 | 32 | 640 | > 5120 | 20 | 20 | 20 | 20 |
| | 20 | 256 | >1024 | >1024 | 640 | 320 | 1.25 | < 0.31 | < 0.31 | >1000 |
| | 30 | 64 | 1024 | >1024 | 1280 | 320 | 10 | 0.63 | < 0.63 | >1000 |
| | 40 | 16 | 1024 | >1024 | 2560 | 160 | 10 | 0.16 | < 0.16 | >1000 |
| | 50 | 32 | 512 | >1024 | 2560 | 320 | 10 | 0.63 | < 0.31 | >1000 |
| | 60 | 32 | 128 | 256 | 640 | 320 | 10 | 2.5 | 1.25 | 420 |
| | 70 | 32 | 64 | 64 | 1280 | 160 | 5 | 2.5 | 2.5 | 392 |

[a] EC = E. coli and PA = P. aeruginosa. [b] $Hc_{10}$ is minimum concentration with less than 10 % hemolysis. [c] $c_H$ is minimum concentration were polymer induced aggregation of red blood cells as observed visually. [d] Selectivity: lowest value among $Hc_{10}$ and $c_H$ divided by MIC value of respective bacteria.

MIC tests revealed a distinct difference between the two investigated topologies. While both polymer types were active against E. coli, the other two bacteria strains were only efficiently inhibited by bottle brush copolymers with MIC values as low as 32 μg mL$^{-1}$. Linear copolymers were only reaching lower inhibition concentrations at high charge densities with a minimum of 64 μg mL$^{-1}$. The tested bottle brush copolymers on the other hand showed a pronounced growth inhibition of all tested bacteria at all charge densities except 20%. In general, antimicrobial activity increased with increasing content of cationic subunits. Similar effects were also observed in previous studies.[17, 30]

The positive effect of multivalent presentation in a bottle brush architecture is remarkable as it was previously reported that an increase in molar mass leads to a decreased antimicrobial activity, especially against gram positive bacteria due to their thicker peptidoglycan layer (cell wall) that was reported to “sieve” out larger macromolecules before they reach the membrane.[44] However, here it is shown that the presented bottle brushes not only show comparable antimicrobial activity against gram negative and gram positive bacteria, they also vastly outperform their linear counterparts, while possessing a molecular weight which is approximately 100 fold increased. It should be noted that compared to linear copolymers, bottle brushes are rather compact, showing a decreased hydrodynamic volume for respective molecular weights. We could also demonstrate that membrane interaction is more efficient for such a multivalent presentation of APs,[45] which, ignoring discrimination by cell wall sieving, fits with the observed decreased MIC values. Overall, bottle brushes show a remarkable broad

band activity against all strains tested, whereas their linear counterparts lack activity for two important strains.

Another important parameter is the compatibility with mammalian cells. Red blood cells (RBCs) are used for this purpose frequently, as they represent the first object an injected polymer would face. To test hemocompatibility hemolysis ($Hc_{10}$) and hemagglutination ($c_H$) tests were performed (**Figure 5**, **S7**, **S8**). The results show distinct differences between bottle brush and linear copolymers. In the tested concentration range (between 40 µg $mL^{-1}$ and 5120 µg $mL^{-1}$) no hemagglutination was observed for bottle brushes while the linear chains led to aggregation of RBCs even at relatively low concentrations around 320 µg $mL^{-1}$. This is in agreement with our previous work where we could demonstrate that the confined nature of side chains in a bottle brush and the limited degrees of freedom, preventing cross linking between liposomes.[45] In contrast, the linear chains perform better comparing the results of hemolysis tests. This effect was expected as multivalence and confinement of bottle brushes leads to increasing membrane activity as also obvious for bacterial cells. In our tests, higher charge densities correlate with lowered hemolytic activity. This impact can be explained by the correlation between hydrophobicity and RBC lysis. [12, 20, 46-48] The best results were achieved for bottle brush BB50, as this was the only polymer which led neither to hemolysis nor hemagglutination in the tested concentration range.

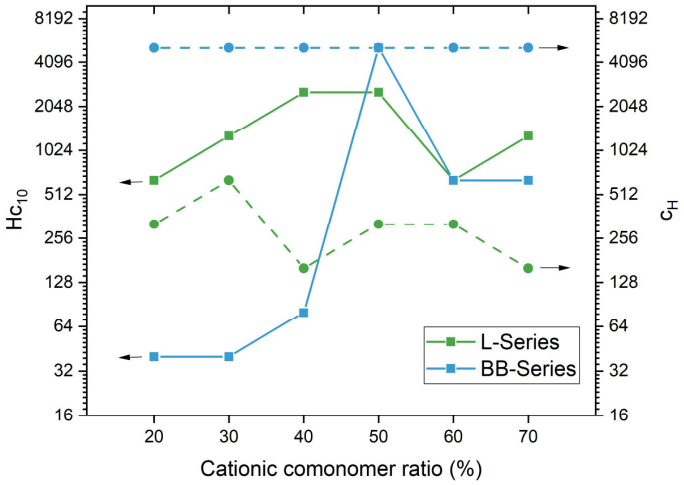


**Figure 5**: Comparison of hemolysis ($Hc_{10}$; square, solid) and hemagglutination ($c_H$; dot, dashed) values of different antimicrobial polymers depending on their architecture and cationic comonomer ratio.

Through determination of blood toxicity and MIC it was possible to calculate the selectivity of investigated copolymers (**Figure 6**) using equation 1 which is a useful benchmark for antimicrobial materials.

$$\text{Selectivity} = \frac{c_H \text{ or } Hc_{10}}{MIC_{50}} \qquad (1)$$

For the calculation the lowest value of either $Hc_{10}$ or $c_H$ was used to reflect the lowest concentration of blood toxicity.

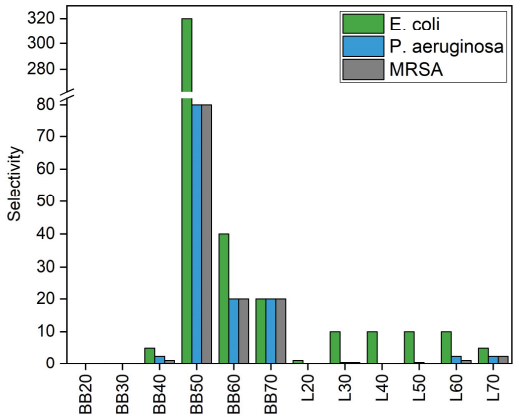


**Figure 6**: Comparison of selectivity against E. coli, MRSA or P. aeruginosa of different antimicrobial polymers depending on their cationic comonomer ratio and architecture.

Considering selectivity, the remarkable improvement of performance when transitioning from a linear to a bottle brush architecture becomes apparent. While linear copolymers show very low values owing to their limited antibacterial activity in combination with their pronounced hemagglutination, bottle brush copolymers above a cationic charge content of 50% show high selectivity values. In particular BB50, with a selectivity around 80 for MRSA and P. Aeruginosa as well as around 320 for E. coli is a promising candidate. Here the combination of membrane activity and the absence of hemotoxicity leads to a pronounced selection of bacterial membranes for tested strains including resistant *Staphylococcus aureus*.

To verify that the shown antibacterial activity is a result of the desired membrane-lytic mechanism we further investigated the performance of the synthesized materials using liposomes, that mimic the composition of different membranes. As such we produced large unilamellar vesicle (LUV)s based on three different phospholipid mixtures representing RBC, E. coli and *Staphylococcus aureus* (SA) respectively. These vesicles were loaded with calcein in a concentration which shows a reduced fluorescence due to self-quenching effects. Upon membrane disruption the concentration of the dye decreases resulting in an increase in fluorescence signal.[50] These constructs were incubated with L50 and BB50, since this composition showed the best results in terms of selectivity. The results (**Figure 7**) reflect the biological data accurately in a qualitative way. Polymers showed membrane permeabilization for both E. coli and SA mimicking LUVs indicating that the cell toxicity is indeed based on membrane disruption. Comparing $EC_{50}$ values between the two polymers also reflects the trend found in MIC values. While there is little difference between the activity of both polymer for E. coli, liposomes mimicking SA are disrupted by BB50 at much lower concentrations compared to L50, which accurately resembles the trend from real bacteria. For RBC mimics no significant dye release was detected within the tested concentration range. This also reflects the findings from hemolysis tests where neither L50 nor BB50 showed a pronounced hemolytic activity. The measurements confirm the membrane activity of herein presented polymers and indicate that the selectivity and activity profile is a function of the varying lipid composition of membranes from different cell types.

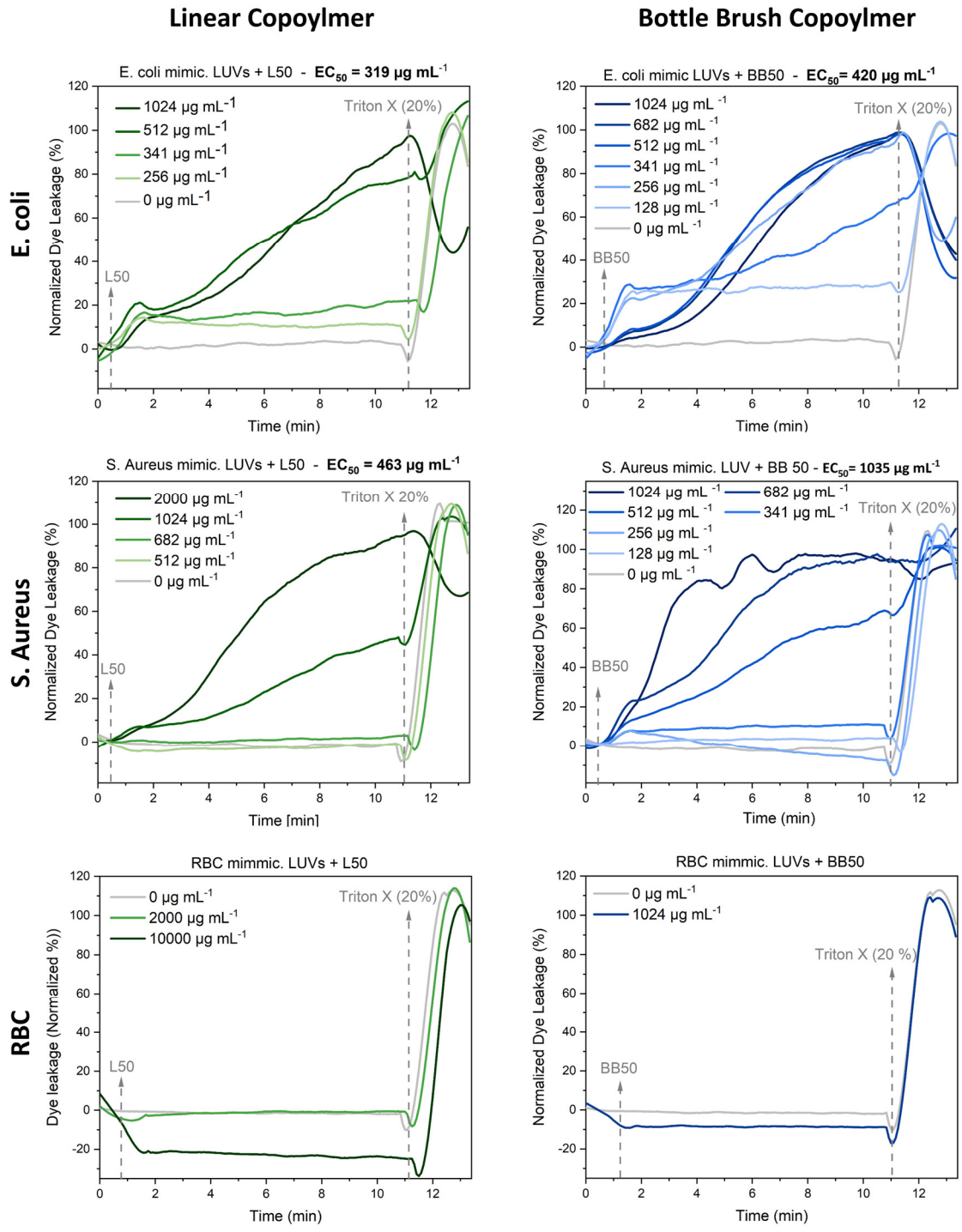


**Figure 7**: Dye leakage studies of BB50 and L50 in combination with LUVs mimicking E. Coli, S. Aureus, and RBC respectively using time resolved fluorescence spectroscopy using an excitation wavelength of 490 nm and an emission wavelength of 525 nm. Dashed arrows indicate addition of polymer at the beginning of each measurement and Triton X at the end. Measurements are normalized to initial fluorescence (0%) and fluorescence after complete release via surfactant addition (100%). $EC_{50}$ values were determined using a Hill fit using Origin software.

A further analysis which is often overlooked in reports dealing with antimicrobial polymers is the cytotoxicity against mammalian cells other than RBCs. However, blood compatibility in such polymers is not necessarily indicating absence of cytotoxicity in general, as shown for linear copolymers, where high charge densities lead to decreased compatibility with human cell lines.[13] To probe our systems we used an MTS assay on HEK cells, which were incubated with various polymer concentrations for 48 h. Cell viability reflects the compatibility of cells with the respective macromolecules (**Figure 8**). Here, linear copolymers are significantly more biocompatible with $IC_{50}$ values above the highest tested concentration (1000 µg $mL^{-1}$) with only two exceptions at high charge densities. Bottle brushes mostly show $IC_{50}$ values below 100 µg $mL^{-1}$ with one exception: BB50. The bottle brush copolymer, which also displays highest selectivity values is also tolerated best by HEK cells under the conditions of the assay. As such the trend regarding toxicity as a function of charge density is similar to hemolysis, but adverse effects are much more pronounced for HEK cells. Microscopic pictures indicate cell lysis under toxic conditions strongly suggesting a membrane lysis responsible for cell death (**Figure S10**). An interesting finding in this regard is the correlation with cationic charge density leading to increased toxicity at high positive charges. This indicates that hydrophobic units might not be as essential for the mode of action of the present polymers. Indeed, the group of Chan-Park described very successful antimicrobial polymers without hydrophobic subunits.[49, 50] Boyer and coworkers reported an increase in cytocompatibility with the introduction of hydrophilic comonomers in ternary polymers.[51] As such, this strategy might also be worth investigating for polymers possessing a bottle brush architecture.

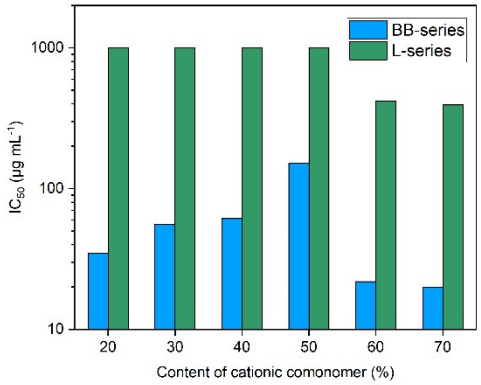


**Figure 8**: Cytotoxicity of antimicrobial polymer possessing a linear or a bottle brush topology, as determined using HEK cells. Cell viability was measured after 48 h incubation with the respective macromolecule at varying concentration using an MTS assay. Measurements were normalized using viability values from untreated cells (100%). Concentration dependent viability values (as a result of triplicates of triplicates) can be found in **Figure S9** and $IC_{50}$ values were determined using a nonlinear fit with variable slope using Prism software.

## Conclusion

In summary, we introduced a new, straight froward way to produce antimicrobial bottle brush copolymers in a one-pot procedure using RAFT polymerization as the sole tool for synthesis of macromolecules. Briefly, polymer featuring hydroxy units in the side chain were functionalized

with CTA molecules and linear antimicrobial building blocks were grafted via RAFT polymerization. Brush synthesis was highly controlled, which in part is attributed to the shuttle approach, producing linear chain alongside grafted structures. Linear polymers can easily be separated from the bottle brush copolymers via precipitation and linear (L-series), as well as brush (BB-series) copolymers were activated via removal of Boc protection groups. To investigate the influence of charge density on the biological activity, polymer with various cationic comonomer contents (20-70%) were produced.

Screening of polymers against three clinically relevant bacteria strains showed a drastic increase in activity for bottle brush structures for both gram-positive and gram-negative bacteria. This is remarkable as literature suggests that especially in the case of gram-positive bacteria, the thick cell wall protects the membrane from polymers when their molecular weight is too high. Blood compatibility gave mixed results as linear chains were highly hemagglutinating, whereas brushes showed hemolysis as main mechanism for toxicity. A bottle brush copolymer with a content of cationic comonomer of 50% (BB50) however was exceptionally hemo-compatible resulting in selectivity values up to 320 for E. Coli and 80 for MRSA and P. Aeruginosa. This trend regarding membrane selectivity was also confirmed artificial membrane model in the form of vesicles.

These excellent results are relativized by a significant incompatibility of polymers of the BB-series with HEK cells, an effect that wasn't detected for linear copolymers. However, also here BB50 showed the highest biocompatibility among bottle brushes. This study further highlights the importance of polymer topology in the context of antimicrobial polymers and how the biological activity of such polymers can be modulated via changes in architecture. The developed synthetic protocol enables us to probe the parameter space of bottle brush copolymers further, for instance in terms of brush length, side chain length, grafting density among others. Also, the introduction of a third monomer type implementing hydrophilic subunits will be investigated in the future.

## Acknowledgement

The authors gratefully acknowledge funding by the German Research Foundation (Deutsche Forschungsgemeinschaft, DFG) (Emmy-Noether-Program, HA 7725/2-1 (A-C.L., A.B., A.A., M.H.). The authors also thank the NMR core facility of the Institute of Chemistry (University of Potsdam) of Prof. Dr. Heiko Möller, Dr. Matthias Heydenreich, and Angela Krtitschka. Prof. Dr. Helmut Schlaad and Sascha Prentzel from the Institute of Chemistry (University of Potsdam) are gratefully acknowledged for providing the facility to perform SEC measurements. M.K. and H.F. acknowledge funding by from the European Union's Horizon 2020 research and innovation programme under grant agreement No 825730

## References

1. Organization, W. H., *Global Antimicrobial Resistance and Use Surveillance System (GLASS) Report*. 2021.

2. English, B. K.; Gaur, A. H., The use and abuse of antibiotics and the development of antibiotic resistance. *Adv Exp Med Biol* **2010,** *659*, 73-82.
3. Love, D. C.; Davis, M. F.; Bassett, A.; Gunther, A.; Nachman, K. E., Dose imprecision and resistance: free-choice medicated feeds in industrial food animal production in the United States. *Environ Health Perspect* **2011,** *119*, 279-83.
4. Balkhair, A., Antibiotics Resistance: When the Armamentarium Gets to the Verge of Being Empty. *Oman Med J* **2017,** *32*, 267-268.
5. Laxminarayan, R.; Duse, A.; Wattal, C.; Zaidi, A. K. M.; Wertheim, H. F. L.; Sumpradit, N.; Vlieghe, E.; Hara, G. L.; Gould, I. M.; Goossens, H.; Greko, C.; So, A. D.; Bigdeli, M.; Tomson, G.; Woodhouse, W.; Ombaka, E.; Peralta, A. Q.; Qamar, F. N.; Mir, F.; Kariuki, S.; Bhutta, Z. A.; Coates, A.; Bergstrom, R.; Wright, G. D.; Brown, E. D.; Cars, O., Antibiotic resistance—the need for global solutions. *The Lancet Infectious Diseases* **2013,** *13*, 1057-1098.
6. Jain, A.; Duvvuri, L. S.; Farah, S.; Beyth, N.; Domb, A. J.; Khan, W., Antimicrobial polymers. *Adv Healthc Mater* **2014,** *3*, 1969-85.
7. Kuroki, A.; Kengmo Tchoupa, A.; Hartlieb, M.; Peltier, R.; Locock, K. E. S.; Unnikrishnan, M.; Perrier, S., Targeting intracellular, multi-drug resistant Staphylococcus aureus with guanidinium polymers by elucidating the structure-activity relationship. *Biomaterials* **2019,** *217*, 119249.
8. Timofeeva, L.; Kleshcheva, N., Antimicrobial polymers: mechanism of action, factors of activity, and applications. *Appl Microbiol Biotechnol* **2011,** *89*, 475-92.
9. Palermo, E. F.; Lee, D.-K.; Ramamoorthy, A.; Kuroda, K., Role of Cationic Group Structure in Membrane Binding and Disruption by Amphiphilic Copolymers. *The Journal of Physical Chemistry B* **2011,** *115*, 366-375.
10. Judzewitsch, P. R.; Zhao, L.; Wong, E. H. H.; Boyer, C., High-Throughput Synthesis of Antimicrobial Copolymers and Rapid Evaluation of Their Bioactivity. *Macromolecules* **2019,** *52*, 3975-3986.
11. Takahashi, H.; Caputo, G. A.; Vemparala, S.; Kuroda, K., Synthetic Random Copolymers as a Molecular Platform To Mimic Host-Defense Antimicrobial Peptides. *Bioconjug Chem* **2017,** *28*, 1340-1350.
12. Phuong, P. T.; Oliver, S.; He, J.; Wong, E. H. H.; Mathers, R. T.; Boyer, C., Effect of Hydrophobic Groups on Antimicrobial and Hemolytic Activity: Developing a Predictive Tool for Ternary Antimicrobial Polymers. *Biomacromolecules* **2020,** *21*, 5241-5255.
13. Kuroki, A.; Sangwan, P.; Qu, Y.; Peltier, R.; Sanchez-Cano, C.; Moat, J.; Dowson, C. G.; Williams, E. G. L.; Locock, K. E. S.; Hartlieb, M.; Perrier, S., Sequence Control as a Powerful Tool for Improving the Selectivity of Antimicrobial Polymers. *ACS Appl. Mater. Interfaces* **2017,** *9*, 40117-40126.
14. Dowling, A. D., J. O' and Adley, C.C. , Antibiotics: Mode of action and meschanisms of resistance. *Antimicrobial research: Novel bioknowledge and educational programs* **2017,** *1*, 536-545.
15. Levy, S. B.; Marshall, B., Antibacterial resistance worldwide: causes, challenges and responses. *Nat Med* **2004,** *10*, S122-9.
16. Knowles, J. R., Penicillin Resistance: The Chemistry of ß-Lactamase Inhibition. *Accounts of Chemical Research* **1985,** *18*, 97-104.
17. Kuroki, A.; Sangwan, P.; Qu, Y.; Peltier, R.; Sanchez-Cano, C.; Moat, J.; Dowson, C. G.; Williams, E. G. L.; Locock, K. E. S.; Hartlieb, M.; Perrier, S., Sequence Control as a Powerful Tool for Improving the Selectivity of Antimicrobial Polymers. *ACS Appl Mater Interfaces* **2017,** *9*, 40117-40126.
18. Palermo, E. F.; Lienkamp, K.; Gillies, E. R.; Ragogna, P. J., Antibacterial Activity of Polymers: Discussions on the Nature of Amphiphilic Balance. *Angew Chem Int Ed Engl* **2019,** *58*, 3690-3693.
19. Ergene, C.; Yasuhara, K.; Palermo, E. F., Biomimetic antimicrobial polymers: recent advances in molecular design. *Polym. Chem.* **2018,** *9*, 2407-2427.
20. Kuroda, K.; Caputo, G. A.; DeGrado, W. F., The role of hydrophobicity in the antimicrobial and hemolytic activities of polymethacrylate derivatives. *Chemistry* **2009,** *15*, 1123-33.

21. Ilker, M. F.; Nüsslein, K.; Tew, G. N.; Coughlin, E. B., Tuning the Hemolytic and Antibacterial Activities of Amphiphilic Polynorbonene Derivates. *Journal of the American Chemical Society* **2004,** *126*, 15870-15875.
22. Palermo, E. F.; Kuroda, K., Chemical Structure of Cationic Groups in Amphiphilic Polymethacrylates Modulates the Antimicrobial and Hemolytic Activities. *Biomacromolecules* **2009,** *10*, 1416-1428.
23. Punia, A.; Debata, P. R.; Banerjee, P.; Yang, N.-L., Structure–property relationships of antibacterial amphiphilic polymers derived from 2-aminoethyl acrylate. *RSC Advances* **2015,** *5*, 95300-95306.
24. Lienkamp, K.; Tew, G. N., Synthetic mimics of antimicrobial peptides--a versatile ring-opening metathesis polymerization based platform for the synthesis of selective antibacterial and cell-penetrating polymers. *Chemistry* **2009,** *15*, 11784-800.
25. Eren, T.; Som, A.; Rennie, J. R.; Nelson, C. F.; Urgina, Y.; Nüsslein, K.; Coughlin, E. B.; Tew, G. N., Antibacterial and Hemolytic Activities of Quaternary Pyridinium Functionalized Polynorbornenes. *Macromol. Chem. Phys.* **2008,** *209*, 516-524.
26. Judzewitsch, P. R.; Nguyen, T. K.; Shanmugam, S.; Wong, E. H. H.; Boyer, C., Towards Sequence-Controlled Antimicrobial Polymers: Effect of Polymer Block Order on Antimicrobial Activity. *Angew Chem Int Ed Engl* **2018,** *57*, 4559-4564.
27. Oda, Y.; Kanaoka, S.; Sato, T.; Aoshima, S.; Kuroda, K., Block versus random amphiphilic copolymers as antibacterial agents. *Biomacromolecules* **2011,** *12*, 3581-91.
28. Lam, S. J.; Wong, E. H.; O'Brien-Simpson, N. M.; Pantarat, N.; Blencowe, A.; Reynolds, E. C.; Qiao, G. G., Bionano Interaction Study on Antimicrobial Star-Shaped Peptide Polymer Nanoparticles. *ACS Appl Mater Interfaces* **2016,** *8*, 33446-33456.
29. Lam, S. J.; O'Brien-Simpson, N. M.; Pantarat, N.; Sulistio, A.; Wong, E. H.; Chen, Y. Y.; Lenzo, J. C.; Holden, J. A.; Blencowe, A.; Reynolds, E. C.; Qiao, G. G., Combating multidrug-resistant Gram-negative bacteria with structurally nanoengineered antimicrobial peptide polymers. *Nat Microbiol* **2016,** *1*, 16162.
30. Laroque, S.; Reifarth, M.; Sperling, M.; Kersting, S.; Klopzig, S.; Budach, P.; Storsberg, J.; Hartlieb, M., Impact of Multivalence and Self-Assembly in the Design of Polymeric Antimicrobial Peptide Mimics. *ACS Appl Mater Interfaces* **2020,** *12*, 30052-30065.
31. Zheng, W.; Anzaldua, M.; Arora, A.; Jiang, Y.; McIntyre, K.; Doerfert, M.; Winter, T.; Mishra, A.; Ma, H.; Liang, H., Environmentally Benign Nanoantibiotics with a Built-in Deactivation Switch Responsive to Natural Habitats. *Biomacromolecules* **2020,** *21*, 2187-2198.
32. Perrier, S., 50th Anniversary Perspective: RAFT Polymerization—A User Guide. *Macromolecules* **2017,** *50*, 7433-7447.
33. Kerr, A.; Hartlieb, M.; Sanchis, J.; Smith, T.; Perrier, S., Complex multiblock bottle-brush architectures by RAFT polymerization. *Chem Commun (Camb)* **2017,** *53*, 11901-11904.
34. Moad, G., RAFT polymerization to form stimuli-responsive polymers. *Polym. Chem.* **2017,** *8*, 177-219.
35. Verduzco, R.; Li, X.; Pesek, S. L.; Stein, G. E., Structure, function, self-assembly, and applications of bottlebrush copolymers. *Chem Soc Rev* **2015,** *44*, 2405-20.
36. Beers, K. L. G., Scott G. and Matyjaszewski, Krzysztof, The Synthesis of Densely Grafted Copolymers by Atom Transfer Radical Polymerization. *Macromolecules* **1998,** *31*, 9413-9415.
37. Moad, G.; Rizzardo, E.; Thang, S., Living Radical Polymerization by the RAFT Process. *Australian Journal of Chemistry* **2005,** *58*, 379-410.
38. Nicolay, R.; Kwak, Y.; Matyjaszewski, K., Dibromotrithiocarbonate Iniferter for Concurrent ATRP and RAFT Polymerization. Effect of Monomer, Catalyst, and Chain Transfer Agent Structure on the Polymerization Mechanism. *Macromolecules* **2008,** *41*, 4585-4596.
39. Zheng, Z.; Ling, J.; Muller, A. H. E., Revival of the R-group approach: a "CTA-shuttled" grafting from approach for well-defined cylindrical polymer brushes via RAFT polymerization. *Macromol Rapid Commun* **2014,** *35*, 234-241.

40. Wang, Y.; Zheng, Z.; Huang, Z.; Ling, J., A CTA-shuttled R-group approach: a versatile synthetic tool towards well-defined functional cylindrical polymer brushes via RAFT polymerization. *Polym. Chem.* **2017,** *8*, 2659-2665.
41. Shanmugam, S.; Cuthbert, J.; Kowalewski, T.; Boyer, C.; Matyjaszewski, K., Catalyst-Free Selective Photoactivation of RAFT Polymerization: A Facile Route for Preparation of Comblike and Bottlebrush Polymers. *Macromolecules* **2018,** *51*, 7776-7784.
42. Lienkamp, K.; Madkour, A. E.; Kumar, K. N.; Nusslein, K.; Tew, G. N., Antimicrobial polymers prepared by ring-opening metathesis polymerization: manipulating antimicrobial properties by organic counterion and charge density variation. *Chemistry* **2009,** *15*, 11715-22.
43. Massey, J. A.; Temple, K.; Cao, L.; Rharbi, Y.; Raez, J.; Winnik, M. A.; Manners, I., Self-Assembly of Organometallic Block Copolymers: The Role of Crystallinity of the Core-Forming Polyferrocene Block in the Micellar Morphologies Formed by Poly(ferrocenylsilane-b-dimethylsiloxane) in n-Alkane Solvents. *J. Am. Chem. Soc.* **2000,** *122*, 11577-11584.
44. Lienkamp, K.; Kumar, K. N.; Som, A.; Nusslein, K.; Tew, G. N., "Doubly selective" antimicrobial polymers: how do they differentiate between bacteria? *Chemistry* **2009,** *15*, 11710-4.
45. Bapolisi, A. M.; Kielb, P.; Bekir, M.; Lehnen, A. C.; Radon, C.; Laroque, S.; Wendler, P.; Muller-Werkmeister, H. M.; Hartlieb, M., Antimicrobial Polymers of Linear and Bottlebrush Architecture: Probing the Membrane Interaction and Physicochemical Properties. *Macromol Rapid Commun* **2022**, e2200288.
46. Palermo, E. F.; Sovadinova, I.; Kuroda, K., Structural Determinants of Antimicrobial Activity and Biocompatibility in Membrane-Disrupting Methacrylamide Random Copolymers. *Biomacromolecules* **2009,** *10*, 3098-3107.
47. Liu, R.; Chen, X.; Chakraborty, S.; Lemke, J. J.; Hayouka, Z.; Chow, C.; Welch, R. A.; Weisblum, B.; Masters, K. S.; Gellman, S. H., Tuning the biological activity profile of antibacterial polymers via subunit substitution pattern. *J Am Chem Soc* **2014,** *136*, 4410-8.
48. Yang, Y.; Cai, Z.; Huang, Z.; Tang, X.; Zhang, X., Antimicrobial cationic polymers: from structural design to functional control. *Polymer Journal* **2017,** *50*, 33-44.
49. Wong, E. H. H.; Khin, M. M.; Ravikumar, V.; Si, Z.; Rice, S. A.; Chan-Park, M. B., Modulating Antimicrobial Activity and Mammalian Cell Biocompatibility with Glucosamine-Functionalized Star Polymers. *Biomacromolecules* **2016,** *17*, 1170-1178.
50. Pranantyo, D.; Xu, L. Q.; Hou, Z.; Kang, E.-T.; Chan-Park, M. B., Increasing bacterial affinity and cytocompatibility with four-arm star glycopolymers and antimicrobial α-polylysine. *Polym. Chem.* **2017,** *8*, 3364-3373.
51. Pham, P.; Oliver, S.; Wong, E. H. H.; Boyer, C., Effect of hydrophilic groups on the bioactivity of antimicrobial polymers. *Polym. Chem.* **2021,** *12*, 5689-5703.